Beyond mean field study of Giant resonances (Gamow-Teller), beta-decay and QCD-based Charge Symmetry Breaking Interaction

Hiroyuki Sagawa RIKEN/University of Aizu

COMEX7
Catania, Italy, June 11-16, 2023

1. Introduction
2. Subtracted second RPA with tensor interactions
3. Gamow-Teller states and quenching problem
4. Magnetic dipole (M1) excitations
5. Beta decay
6. QCD-based CSB and Okamoto-Nolen-Schiffer anomaly
7. Summary

Beyond mean field model

Particle –vibration coupling model (RPA+ PVC)
Quasi-particle RPA+PVC (QRPA+QPVC)
Relativistic quasiparticle time blocking approximation (RQTBA)
Second RPA model (SQRA)
Subtracted SRPA model. (SSRPA)
Generator coordinate model (GCM)

G. Colo
Yifei Niu, Monday

D. Gambacarta, today
E. Letvinova, Friday

Today's topics
SSRPA for Gamow-Teller giant resonance and beta decay

Targets of Second RPA

- Spreading width of giant resonances
- Quenching of spin-isospin excitations.
- Low-energy pigmy states

SSRPA is based on a proper idea of the EDF theory since it is designed for the mean field model applications (HF, RPA).

SRPA phonon operator

$$Q_\nu^\dagger = \sum_{ph}(X^\nu_{ph} a^\dagger_p a_h - Y^\nu_{ph} a^\dagger_h a_p) + \sum_{\substack{p_1<p_2\\h_1<h_2}} (X^\nu_{p_1p_2h_1h_2} a^\dagger_{p_1} a^\dagger_{p_2} a_{h_2} a_{h_1} - Y^\nu_{p_1p_2h_1h_2} a^\dagger_{h_1} a^\dagger_{h_2} a_{p_2} a_{p_1})$$

RPA ground state is defined as

$$|\Psi\rangle = e^{\hat{S}}|\Phi\rangle,$$

where

$$\hat{S} = \sum_{ph} C_{ph}(t) a^\dagger_p a_h,$$

SRPA operator is

$$\hat{S} = \sum_{ph} C_{ph}(t) a^\dagger_p a_h + \frac{1}{2}\sum_{php'h'} \hat{C}_{pp'hh'}(t) a^\dagger_p a^\dagger_{p'} a_h a_{h'}.$$

Equation of motion give SRPA matrix equation

$$[H, Q^\dagger] = \hbar\omega Q^\dagger$$

The basic idea is the same as the coupled cluster model with singlet (s)- and doublet (d)- pairs.

RPA equation.

$$\begin{bmatrix} A & B \\ -B^* & -A^* \end{bmatrix} \begin{bmatrix} X^\nu \\ Y^\nu \end{bmatrix} = \hbar\omega_\nu \begin{bmatrix} X^\nu \\ Y^\nu \end{bmatrix}$$

$$A = \begin{pmatrix} A_{11} & A_{12} \\ A_{21} & A_{22} \end{pmatrix}, B = \begin{pmatrix} B_{11} & B_{12} \\ B_{21} & B_{22} \end{pmatrix}$$

$$X = \begin{pmatrix} X_1^\nu \\ X_2^\nu \end{pmatrix}, Y = \begin{pmatrix} Y_1^\nu \\ Y_2^\nu \end{pmatrix}$$

$$\begin{aligned} A_{11} =& A_{ph;p'h'} \\ =& < HF|[a_h^\dagger a_p, [H, a_{p'}^\dagger a_{h'}]]|HF > \\ =& (E_p - E_h)\delta_{pp'}\delta_{hh'} + \bar{V}_{ph'hp'} \end{aligned}$$

$$\begin{aligned} B_{11} =& B_{ph;p'h'} \\ =& - < HF|[a_h^\dagger a_p, [H, a_{h'}^\dagger a_{p'}]]|HF > \\ =& \bar{V}_{pp'hh'} \end{aligned}$$

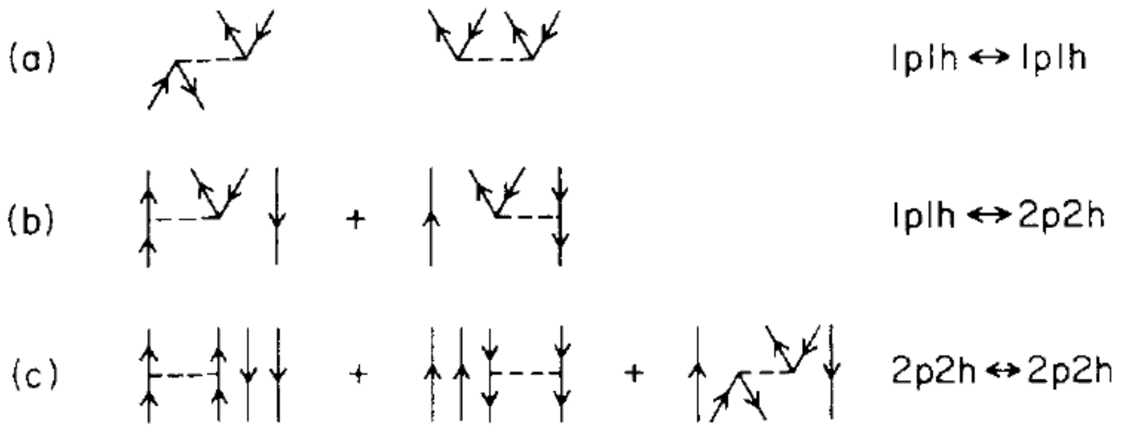

$$\begin{aligned} A_{12} =& A_{ph;p_1p_2h_1h_2} \\ =& < HF|[a_h^\dagger a_p, [H, a_{p_1}^\dagger a_{p_2}^\dagger a_{h_2} a_{h_1}]]|HF > \\ =& U(h_1h_2)\bar{V}_{p_1p_2ph_2}\delta_{hh_1} - U(p_1p_2)\bar{V}_{hp_2h_1h_2}\delta_{pp_1} \end{aligned}$$

$U(h_1h_2)$ is an anti-symmtrizer.

$$\begin{aligned} A_{22} =& A_{p_1p_2h_1h_2;p_1'p_2'h_1'h_2'} \\ =& < HF|[a_{h_1}^\dagger a_{h_2}^\dagger a_{p_2} a_{p_1}, [H, a_{p_1'}^\dagger a_{p_2'}^\dagger a_{h_2'} a_{h_1'}]]|HF > \\ =& (E_{p_1} + E_{p_2} - E_{h_1} - E_{h_2})U(p_1p_2)U(h_1h_2) \\ & \times \delta_{p_1p_1'}\delta_{p_2p_2'}\delta_{h_1h_1'}\delta_{h_2h_2'} \\ & + U(h_1h_2)\bar{V}_{p_1p_2p_1'p_2'}\delta_{h_1h_1'}\delta_{h_2h_2'} \\ & + U(p_1p_2)\bar{V}_{h_1h_2h_1'h_2'}\delta_{p_1p_1'}\delta_{p_2p_2'} \\ & - U(p_1p_2)U(h_1h_2)U(p_1'p_2')U(h_1'h_2') \\ & \times \bar{V}_{p_1h_1'p_1'h_1}\delta_{p_2p_2'}\delta_{h_2h_2'} \end{aligned}$$

In SRPA with subtraction procedure (SSRPA), A_{11} and B_{11} are modified.

$$
\begin{aligned}
A^S_{11'} =& A_{11'} + \sum_2 A_{12}(A_{22})^{-1}A_{21'} + \sum_2 B_{12}(A_{22})^{-1}B_{21'} \\
B^S_{11'} =& B_{11'} + \sum_2 A_{12}(A_{22})^{-1}B_{21'} + \sum_2 B_{12}(A_{22})^{-1}A_{21'}
\end{aligned}
$$

$$
\mathcal{A}^S_F = \begin{pmatrix} A_{11'} + \sum_{2,2'} A_{12}(A_{22'})^{-1}A_{2'1'} + \sum_{2,2'} B_{12}(A_{22'})^{-1}B_{2'1'} & A_{12} \\ A_{21} & A_{22'} \end{pmatrix},
$$

$$
\mathcal{B}^S_F = \begin{pmatrix} B_{11'} + \sum_{2,2'} A_{12}(A_{22'})^{-1}B_{2'1'} + \sum_{2,2'} B_{12}(A_{22'})^{-1}A_{2'1'} & B_{12} \\ B_{21} & 0 \end{pmatrix}.
$$

PHYSICAL REVIEW C **106**, 014319 (2022)

Gamow-Teller transitions in magic nuclei calculated by the charge-exchange subtracted second random-phase approximation

M. J. Yang,[1] C. L. Bai,[1] H. Sagawa,[2,3] and H. Q. Zhang[4]

Skyrme tensor interactions

$$v_T = \frac{T}{2}\left\{\left[(\vec{\sigma}_1\cdot k')(\vec{\sigma}_2\cdot k') - \frac{1}{3}(\vec{\sigma}_1\cdot\vec{\sigma}_2)k'^2\right]\delta(\vec{r}_1-\vec{r}_2) + \delta(\vec{r}_1-\vec{r}_2)\left[(\vec{\sigma}_1\cdot k)(\vec{\sigma}_2\cdot k) - \frac{1}{3}(\vec{\sigma}_1\cdot\vec{\sigma}_2)k^2\right]\right\}$$
$$+ U\left\{(\vec{\sigma}_1\cdot k')\delta(\vec{r}_1-\vec{r}_2)(\vec{\sigma}_2\cdot k) - \frac{1}{3}(\vec{\sigma}_1\cdot\vec{\sigma}_2)\left[k'\cdot\delta(\vec{r}_1-\vec{r}_2)k\right]\right\},$$

Mean field potential

$$h_{so} = U_{so}\, l\cdot\sigma$$

$$\boxed{\alpha_T = \frac{5}{12}U}$$

$$\boxed{\beta_T = \frac{5}{24}(T+U)}$$

$$U_{so} = \frac{W_0}{r}\left(\frac{d\rho_q}{dr} + \frac{d\rho_{1-q}}{dr}\right) + \alpha\frac{J_q}{r} + \beta\frac{J_{1-q}}{r}$$

$$J_q(r) = \frac{1}{4\pi r^3}\sum_{i\in q} v_i^2(2j_i+1)\left[j_i(j_i+1) - l_i(l_i+1) - \frac{3}{4}\right]R_i^2(r)$$

$$q = 0\ neutron$$
$$= 1\ proton$$

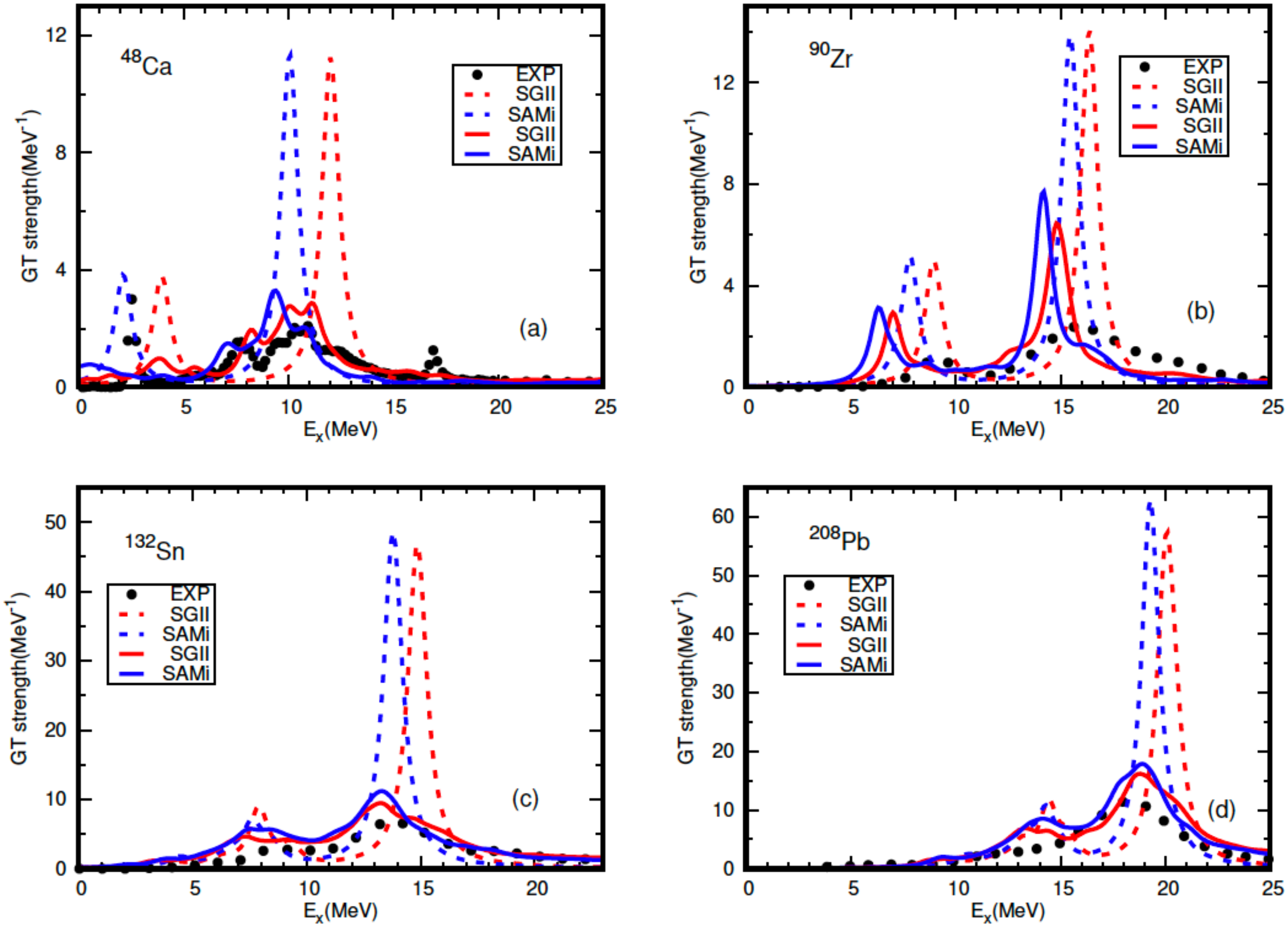

Dashed line RPA
Solid line SSRPA

SGII and SAMi are specially designed for spin-isospin excitations (Landau parameter g')

FIG. 3: GT$_-$ strength distributions of ^{48}Ca [panel (a)], ^{90}Zr [panel (b)], ^{132}Sn [panel (c)] and ^{208}Pb [panel (d)] calculated with the SGII and SAMi EDFs by RPA (dash lines) and SSRPA (solid lines). The results obtained by SGII and SAMi are shown by the red and blue lines, respectively. The experimental data of ^{48}Ca [41], ^{90}Zr [42], ^{132}Sn [43], and ^{208}Pb [44] are shown by the black filled circles. The calculated discrete strength distributions are smoothed by a Lorentzian weighting function of 1 MeV

Phys. Rev. C 106, 014319/pp. 1-10 (2022) - (Published 28 July 2022)

Te1 (T,U)=(500, -350) Te2 (600, 0) Te3 (650, 200)

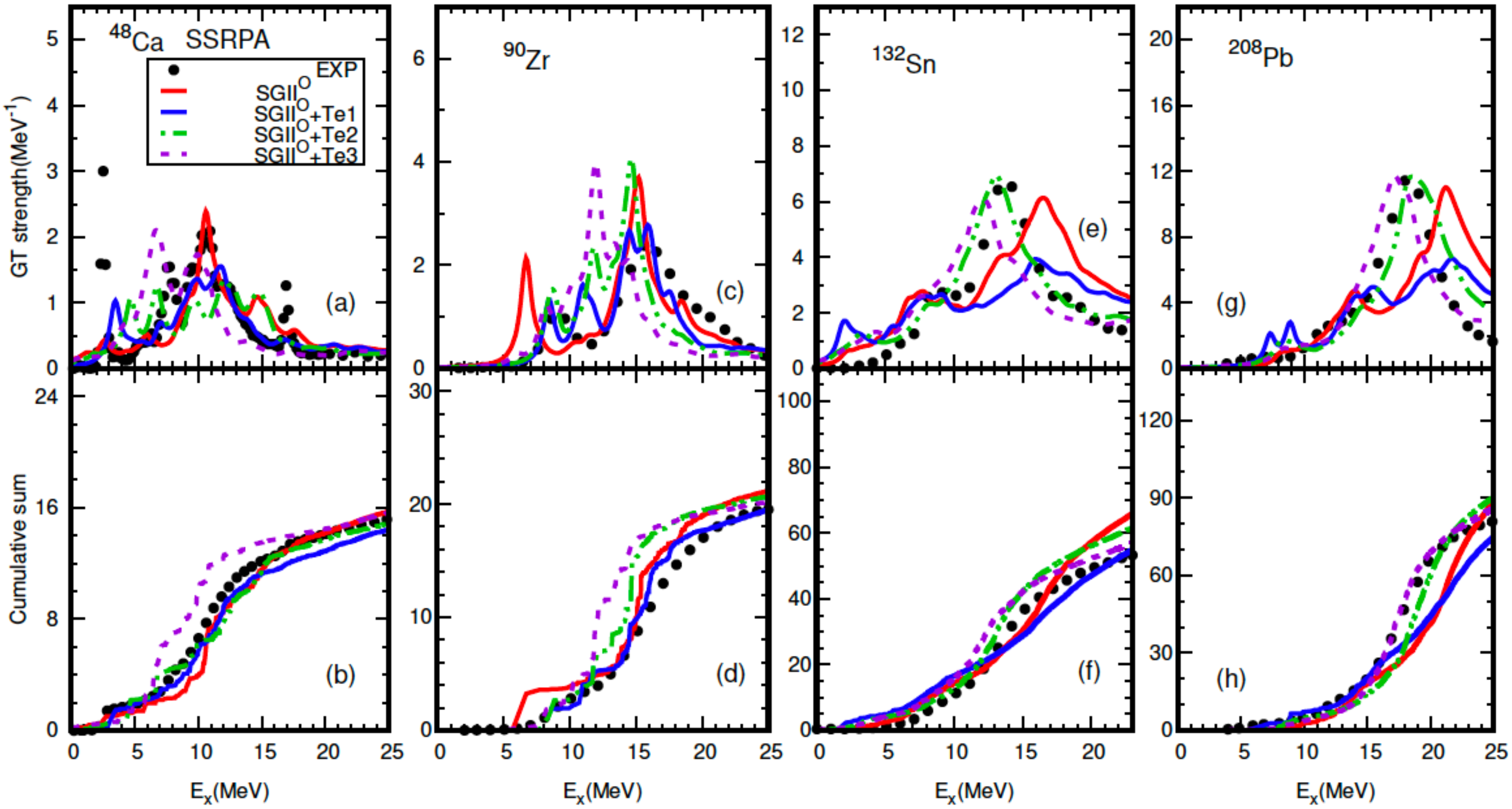

The quenching factor of Gamow-Teller strength

The cumulative sums are taken up to E_{max} = 25 MeV for ^{48}Ca and ^{90}Zr, 23 MeV for ^{132}Sn, and 25 MeV for ^{208}Pb,

Force	(T,U)	^{48}Ca	^{90}Zr	^{132}Sn	^{208}Pb
SAMi	(0,0)	14.4%	15.2%	12.5%	10.0%
SAMi-T	(415.5,-95.5)	18.6%	16.3%	14.2%	12.7%
SGII^{O}	(0,0)	34.4%	29.4%	31.4%	33.2%
SGII^{O}+Te1	(500,-350)	39.8%	35.0%	42.8%	43.2%
SGII^{O}+Te2	(600, 0)	37.9%	31.0%	35.8%	31.7%
SGII^{O}+Te3	(650,200)	34.8%	32.6%	40.6%	35.0%
Exp.		36.7 %	34.9 %	44.5%	38.6 %

SAMi-T: tensor 1-4% more quenching
SGII+Te1: tensor 5-10 % more quenching

Triplet-odd tensor plays an effective role to
Increase the quenching.

Magnetic dipole transitions and $M(\sigma\tau)$ strength in ^{48}Ca and ^{90}Zr in SSRPA

Mingjun Yang, Chunlin Bai and HS

Triplet-odd tensor for the spin-orbit splitting of p-h excitations of the same particles

Preliminary

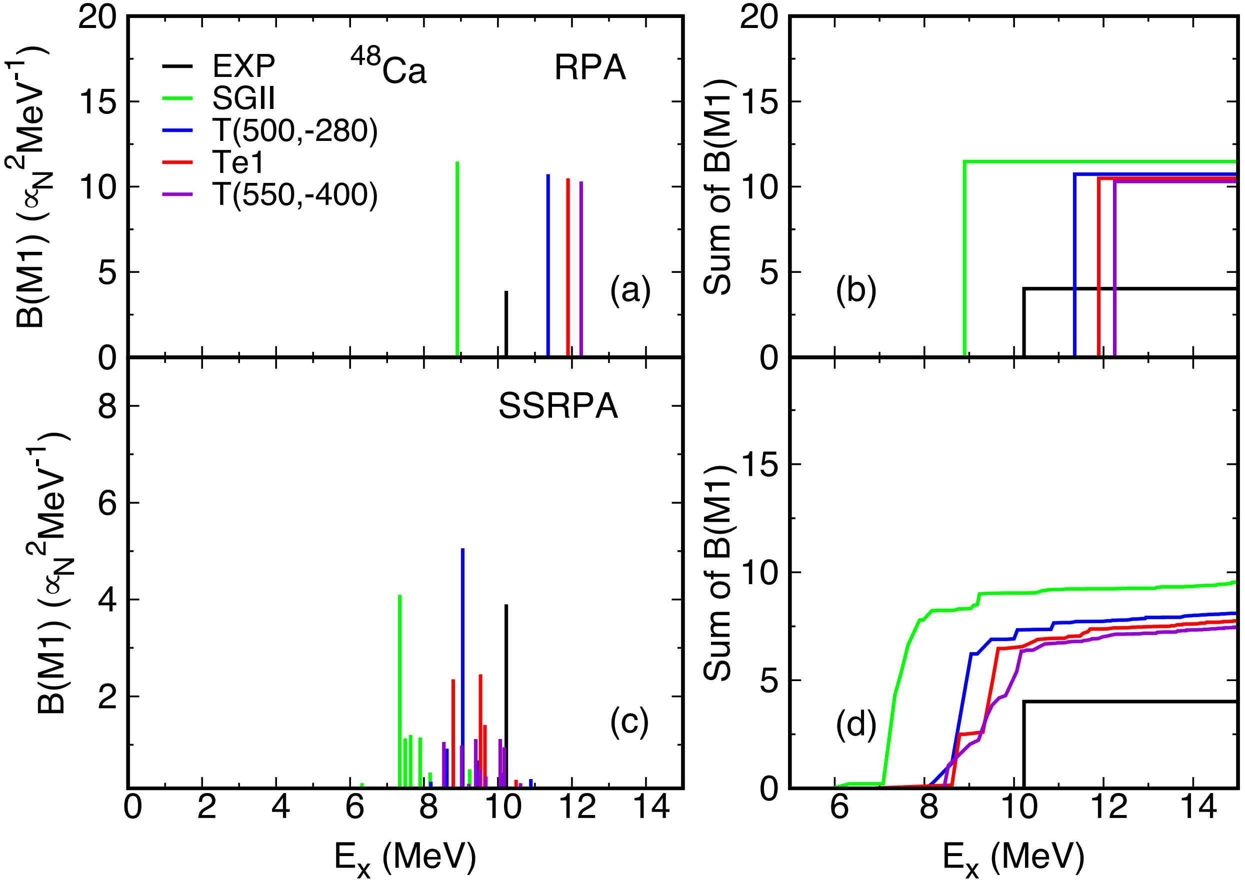

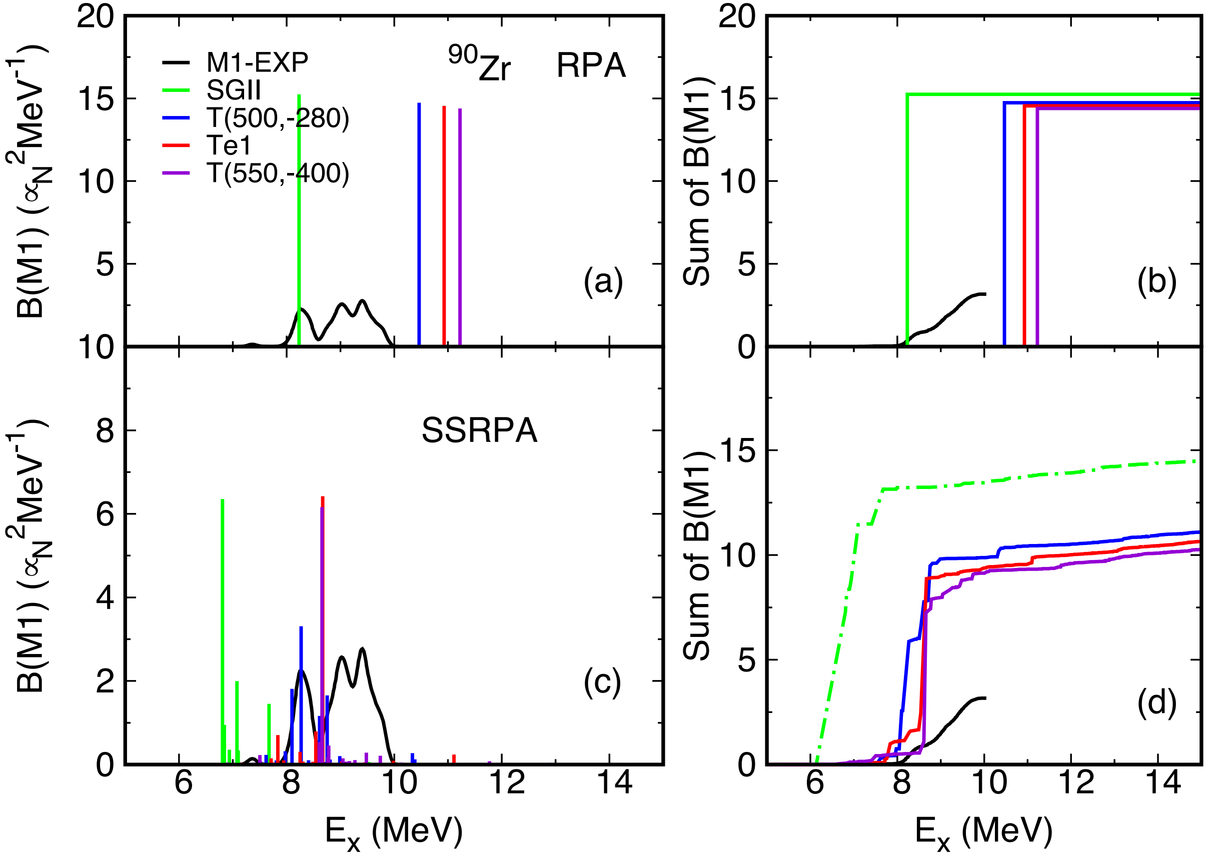

Te1=(500,-350)

$$\boxed{U_{so} = \frac{W_0}{r}\left(\frac{d\rho_q}{dr} + \frac{d\rho_{1-q}}{dr}\right) + \alpha\frac{J_q}{r} + \beta\frac{J_{1-q}}{r}}$$

$$\boxed{\alpha_T = \frac{5}{12}U}$$

nagative U gives larger spin − orbit for M1

TABLE III: The excitation energy of 1^+ state in ^{90}Zr. The energy is calculated with SGII+(T,U)=(500,-280) and SAMi-T,(T,U)=(415.5,−91.4). Δ E^T is the difference of energy between with and without the tensor interaction. The experimental energy is ∼9.0 MeV. The unit is in MeV.

Excitation Energy

SGII+(T,U)	HF	RPA	ΔE(RPA-HF)	SSRPA	ΔE(SSRPA-HF)
w/o	6.21	8.23	2.02	6.81	0.60
with	8.77	10.46	1.69	8.27	−0.50
Δ E^T	2.56	2.23		1.46	
SAMi-T+(T,U)	HF	RPA	ΔE(RPA-HF)	SSRPA	ΔE(SSRPA-HF)
w/o	6.25	8.42	2.17	7.52	1.27
with	7.05	9.19	2.14	8.20	1.15
Δ E^T	0.80	0.77		1.68	

B(M1) strength

SGII+(T,U)	HF	RPA	SSRPA
w/o	15.53	15.24 (98.1%)	12.56 (80.9%)
with		14.73 (94.8%)	10.93 (70.4%)
ΔB^T		-0.51 (3.2 %)	-1.63 (10.5 %)
SAMi-T+(T,U)	HF	RPA	SSRPA
w/o	15.53	15.37 (99.1%)	13.27 (85.4%)
with		15.22 (98.0%)	13.05 (84..0%)
ΔB^T		-0.15 (1.1%)	-0.22 (1.4%)

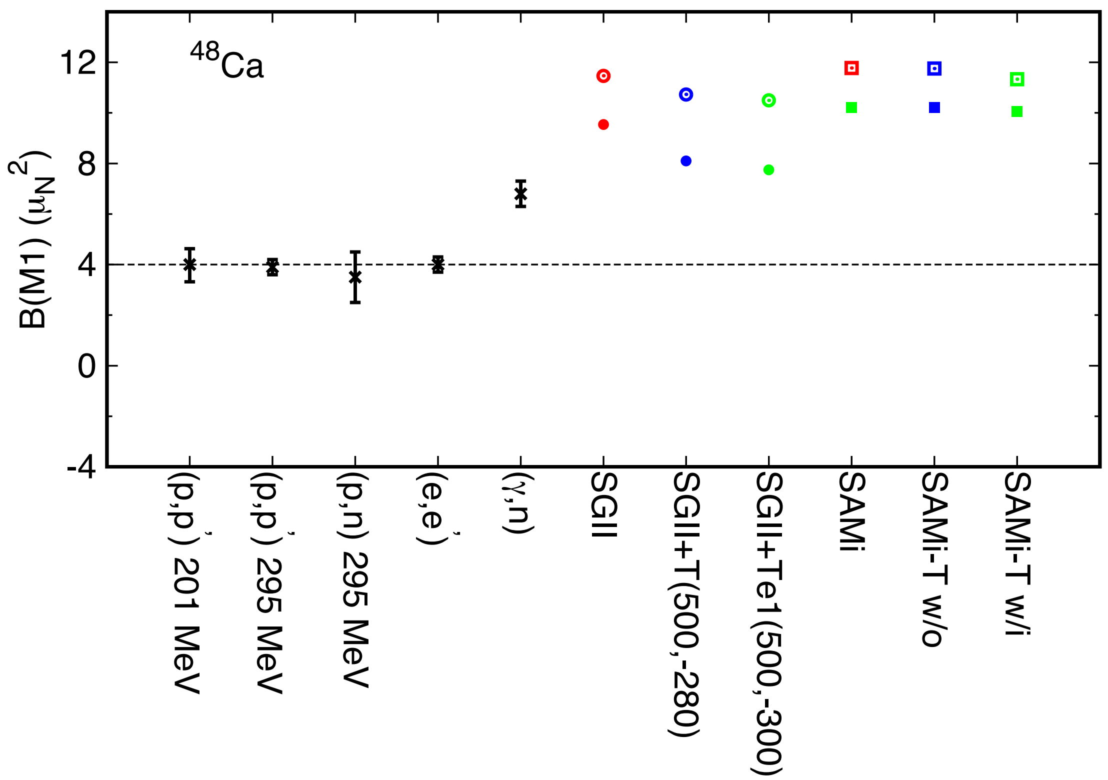

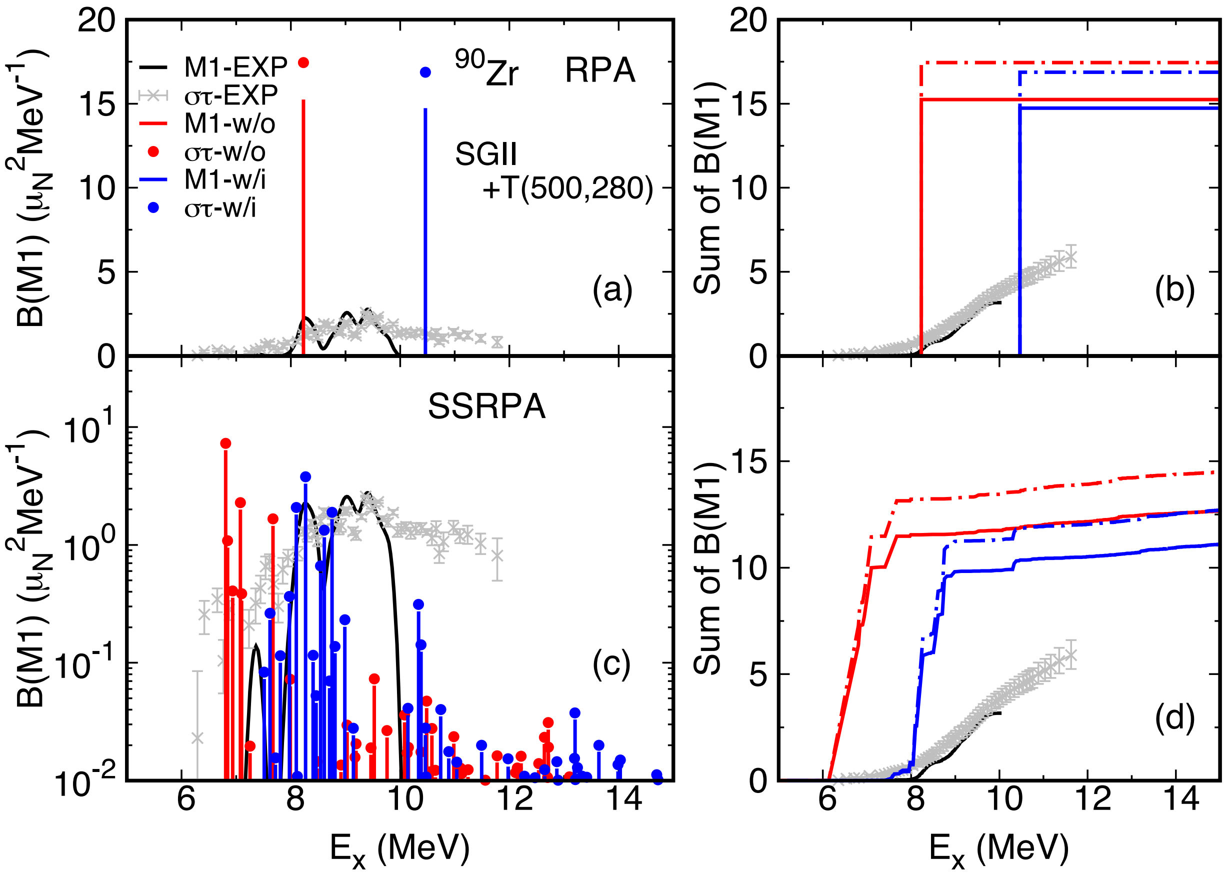

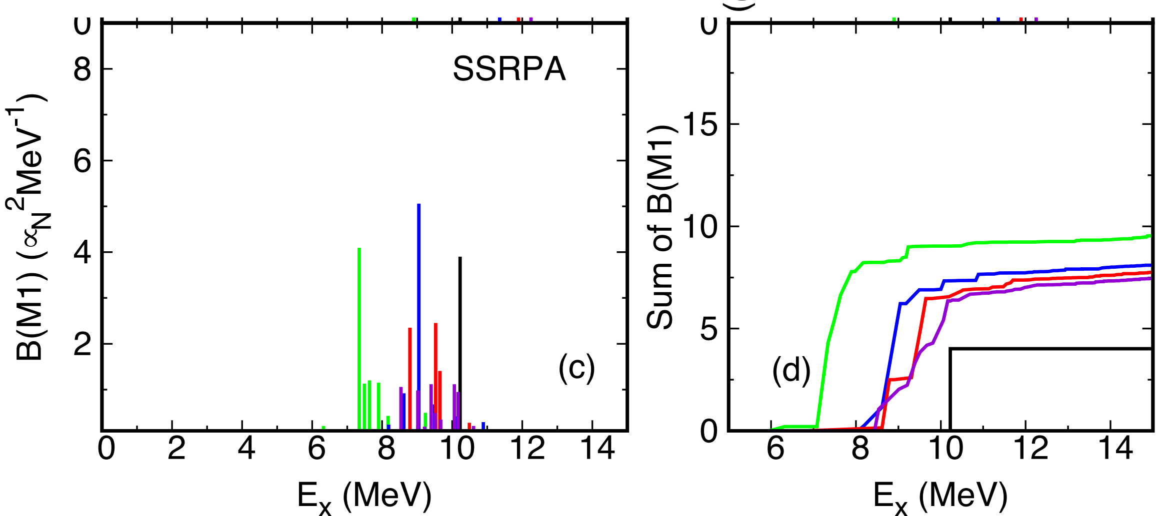

Iwamoto, Tamii (p,p')

Beyond mean field study of Giant resonances (Gamow-Teller), beta-decay and QCD-based Charge Symmetry Breaking Interaction

Hiroyuki Sagawa RIKEN/University of Aizu

COMEX7
Catania, Italy, June 11-16, 2023

1. Introduction
2. Subtracted second RPA with tensor interactions
3. Gamow-Teller states and quenching problem
4. Magnetic dipole (M1) excitations
5. Beta decay
6. QCD-based CSB and Okamoto-Nolen-Schiffer anomaly
7. Summary

Effects of two particle-two hole configurations and tensor force on β decay of magic nuclei

M. J. Yang,[1] H. Sagawa,[2,3] C. L. Bai,[1] and H. Q. Zhang[4]

[1] *College of Physics, Sichuan University, Chendu 610065, China*
[2] *Center for Mathematics and Physics, University of Aizu, Aizu-Wakamatsu, Fukushima 965-8560, Japan*
[3] *RIKEN, Nishina Center, Wako 351-0198, Japan*
[4] *China Institute of Atomic Energy, Beijing 102413, China*

Phys. Rev. C **107**, 014325 (2023) - Published 30 January 2023

$$B^{GT\pm}_{1^+_n} = | < 1^+_n || \hat{O}^{\pm}_{GT} || 0 > |^2,$$

$$\hat{O}^{\pm}_{GT} = \sum_{i=1}^{A} \sigma(i) t_{\pm}(i),$$

$$T_{1/2} = \frac{D}{g_A^2 \sum_n^{\Delta_n H} B^{GT-}_{1^+_n} f_0(Z, A, \omega_n)},$$

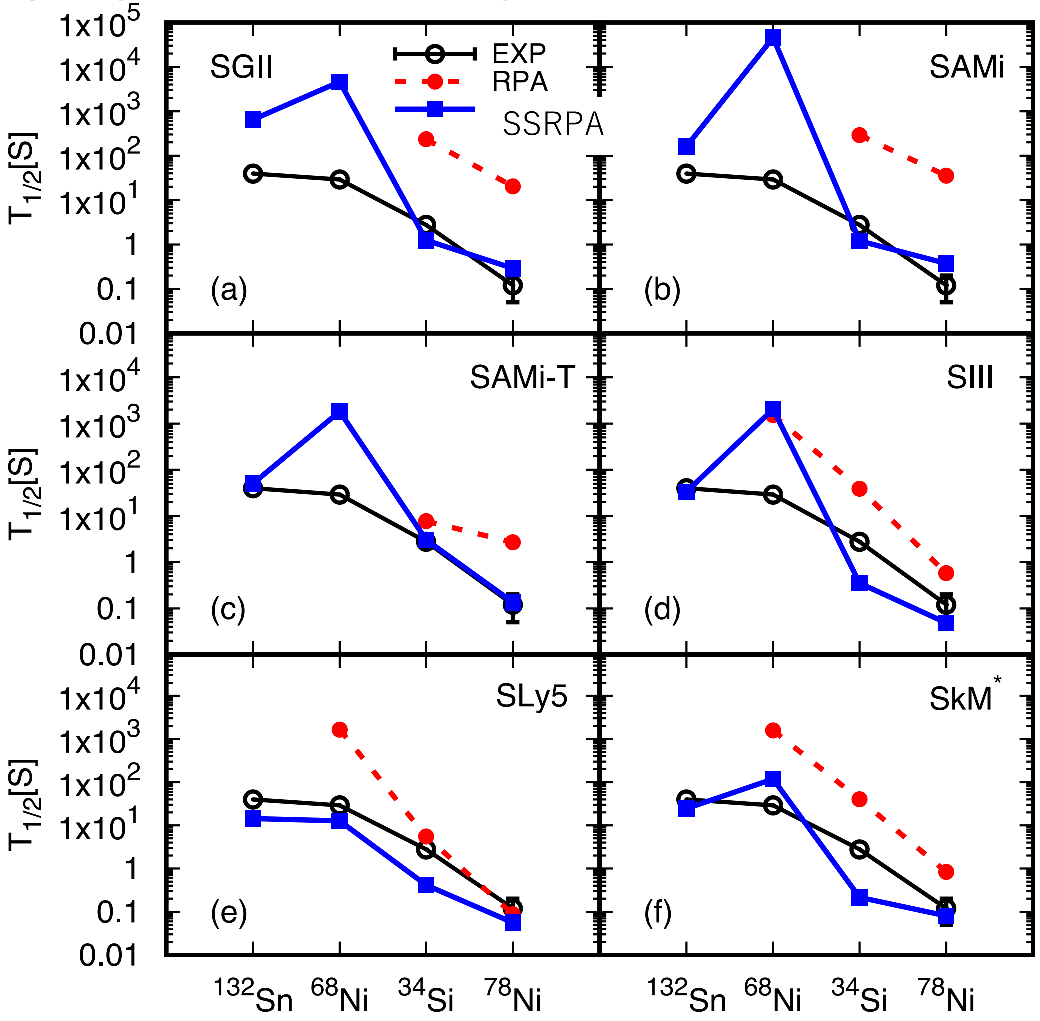

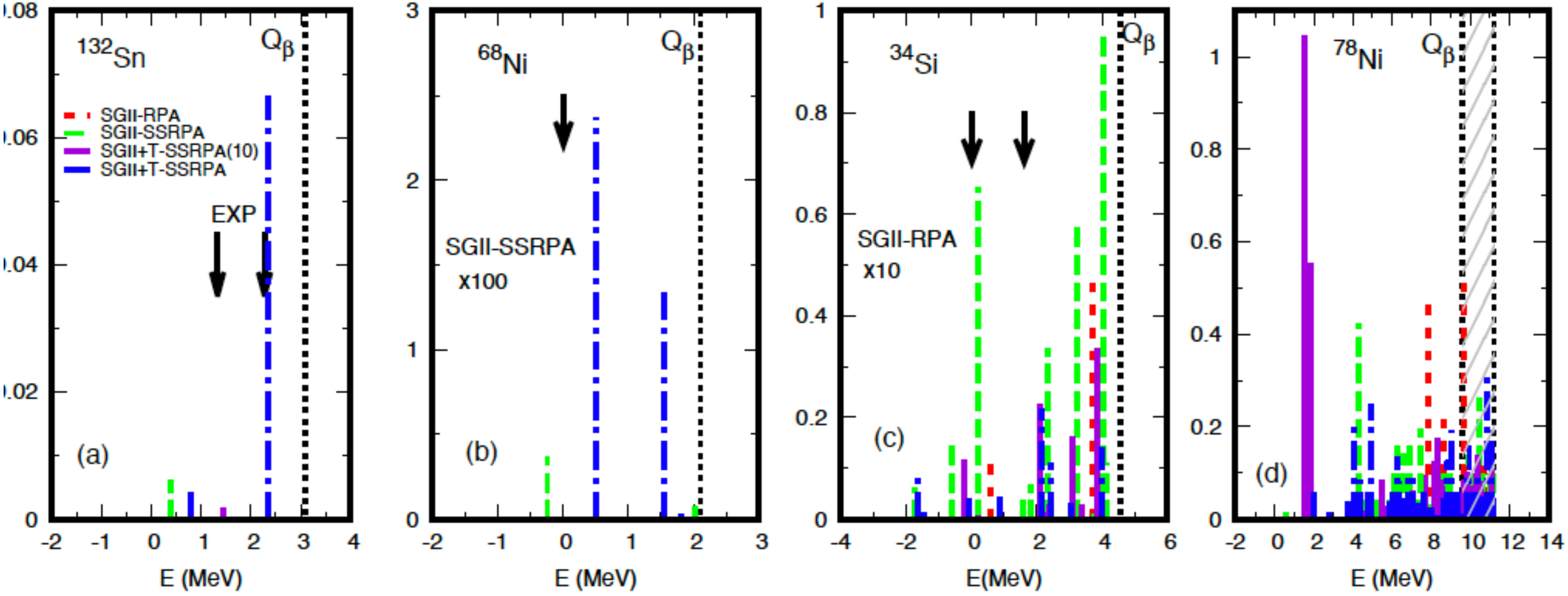

FIG. 5: The GT strength distributions with respect to the daughter nucleus in ^{132}Sn, ^{68}Ni, ^{34}Si, and ^{78}Ni calculated by RPA with SGII and SSRPA with SGII and SGII+T. The observed excitation energies of GT states are marked by the arrows [13].

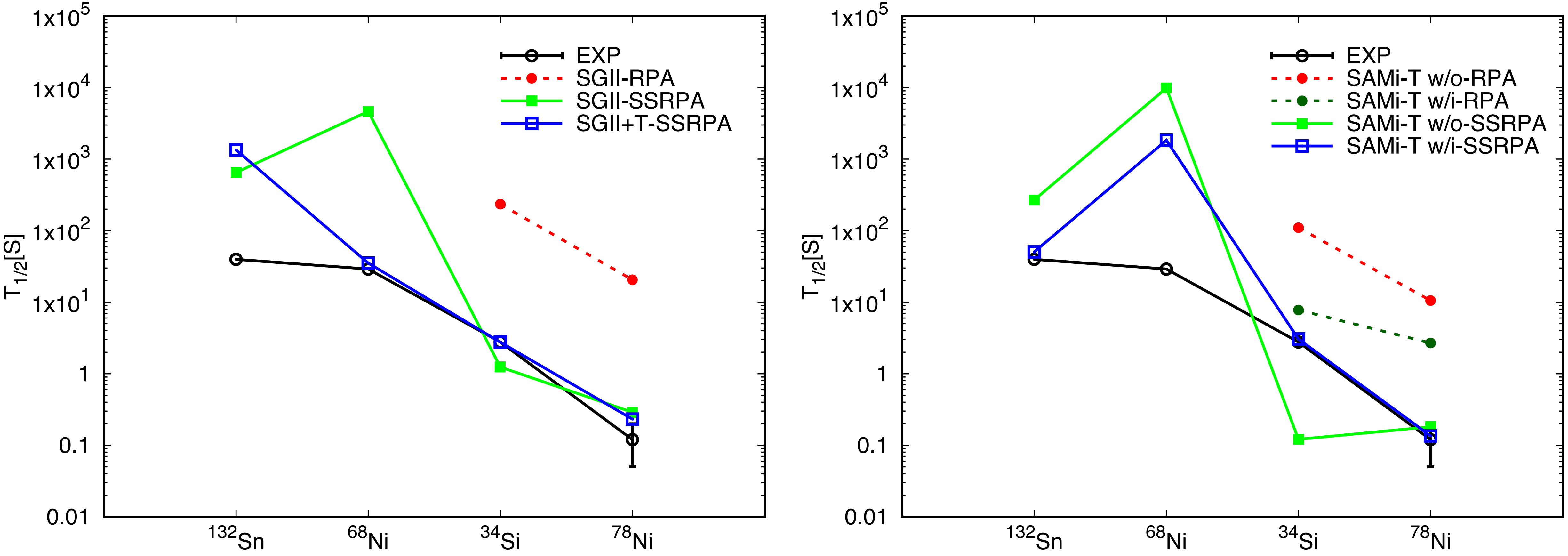

EXP
SGII-RPA
SGII-SSRPA
SGII+T-SSRPA
T1/2[S]
1x10^5
1x10^4
1x10^3
1x10^2
1x10^1
1
0.1
0.01
132Sn
68Ni
34Si
78Ni
EXP
SAMi-T w/o-RPA
SAMi-T w/i-RPA
SAMi-T w/o-SSRPA
SAMi-T w/i-SSRPA

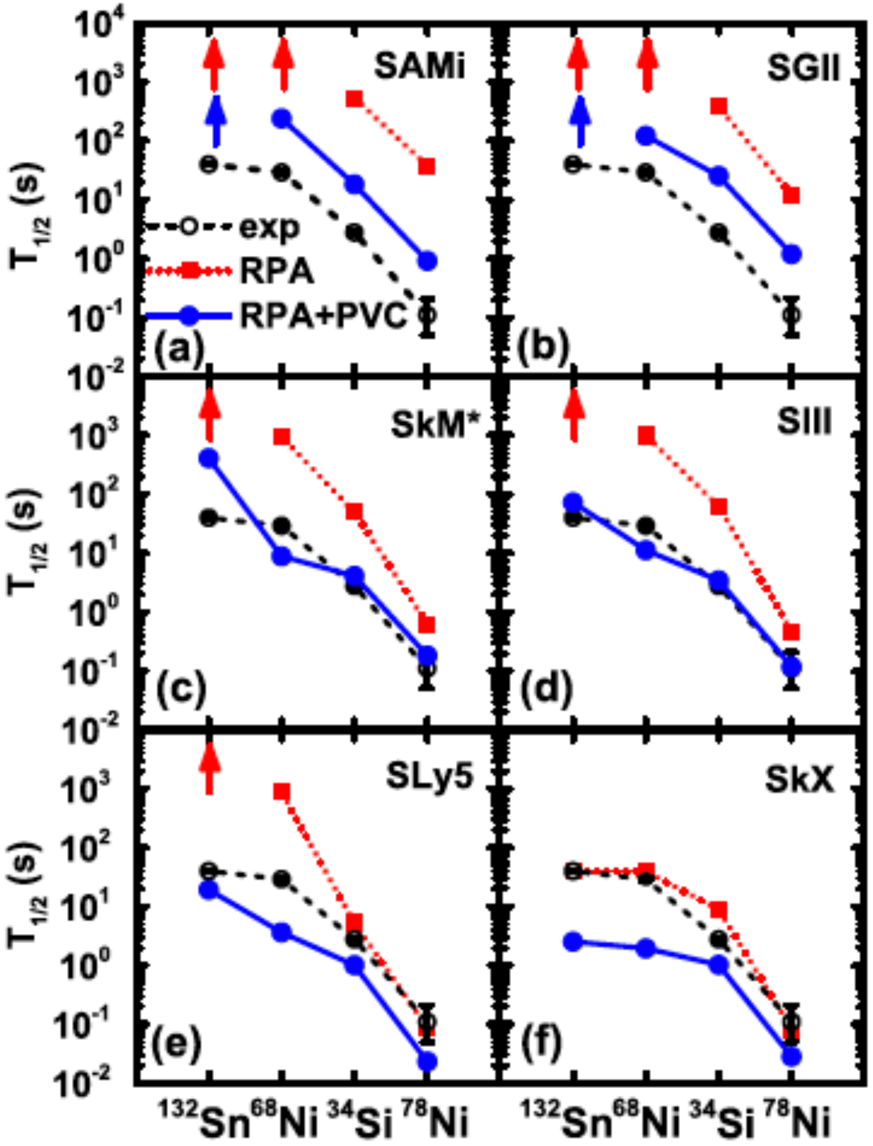

Niu, Colo et al., RPA+PVC

PRL **114**, 142501 (2015)

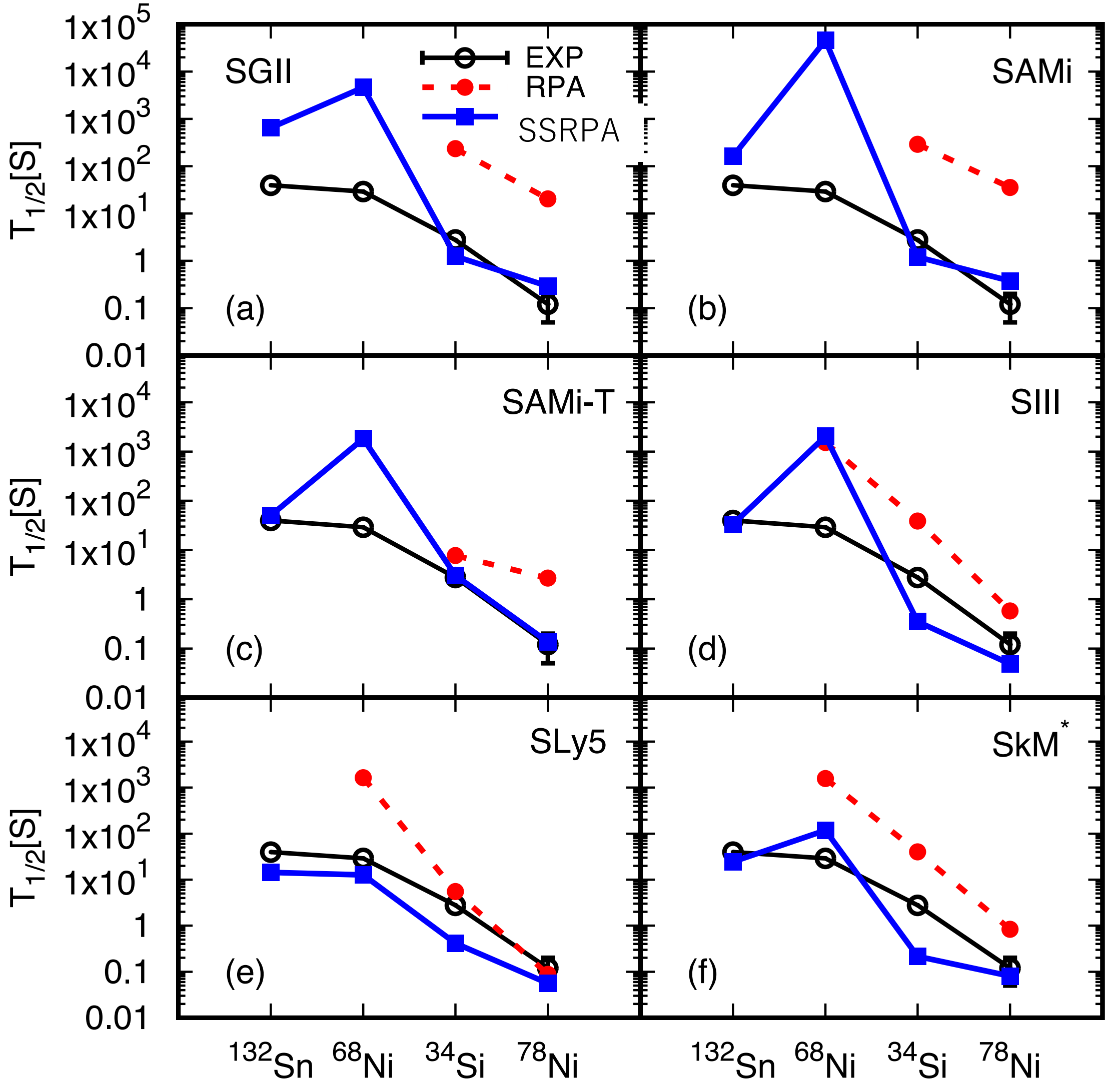

SSRPA

Beyond mean field study of Giant resonances (Gamow-Teller), beta-decay and QCD-based Charge Symmetry Breaking Interaction

Hiroyuki Sagawa RIKEN/University of Aizu

COMEX7
Catania, Italy, June 11-16, 2023

1. Introduction
2. Subtracted second RPA with tensor interactions
3. Gamow-Teller states and quenching problem
4. Magnetic dipole (M1) excitations
5. Beta decay
6. QCD-based CSB and Okamoto-Nolen-Schiffer anomaly
7. Summary

T. Naito, this morning

RIKEN NiSHiNA CENTER

to Advance Knowledge for Humanity THE UNIVERSITY OF AIZU 1993

Isospin Breaking Interactions (ISB)

Concept of Isospin proposed by J. Heisenberg, 1932 and E. P. Wigner, 1937

Isospin conservation $[H,T]=0$

$$[H,T]=[V_C+V_{CSB}+V_{CIB},T]\neq 0$$

charge symmetry breaking
$V_{CSB}=V_{nn}-V_{pp}$

Charge independence breaking
$V_{CIS}=(V_{nn}+V_{pp})/2-V_{np}$

Scattering Length

$$a^{pp}_{(S=0)} = -17.3\pm0.4\text{fm},$$
$$a^{nn}_{(S=0)} = -18.7\pm0.6\text{fm}, \quad (5.4)$$
$$a^{pn}_{(S=0)} = -23.70\pm0.03\text{fm}.$$

The difference between a_0^{pp} and a_0^{nn} is an evidence of CSB (charge symmetry breaking) nuclear force, while the difference between a_0^{pn} and the average $(a_0^{pp}+a_0^{nn})/2$ is due to CIB (charge invariance breaking) force. These negative

QCD-based Charge Symmetry Interaction and Okamoto-Nolen-Schiffer anomaly

HS, T. Naito, X. Roca-Maza and T. Hatsuda, aarXiv/2305.17481 in nucl-theory r

[Okamoto-Nolen-Schiffer anomaly]
Coulomb energy differences between mirror nuclei and Isobaric analogue states from A=3~220 are always 3-9 % larger than theoretical calculations of Independent particle model.

This anomaly suggests
1) 10-20% smaller proton radii of valence particles than those of core
2) The effect of Charge symmetry interaction (CSB)

Standard model on CSB interactions
1) Meson exchange model sigma-rho and pi-eta meson exchange potentials.
2) Phenomenological Skyrme EDF to reproduce ground state properties of mirror nuclei.

QCD –based approach

Proton=(uud) $m_u c^2 \sim 2.3$MeV
Neutron=(udd) $m_d c^2 \sim 4.8$MeV
Explicit Chiral symmetry breaking
QCD dynamics of strong interaction
(Spontaneous chiral symmetry breaking)

QCD-based CSB interaction

1. QCD sum rule approach to evaluate mass difference of proton and neutron in nuclear medium
2. Partial restoration of Spontaneous symmetry breaking (SSB) in nuclear medium

The binding energy (mass) of neutron and proton is formulated in nuclear matter by the QCD sum rule approach in leading order of the quark mass difference and QED effect

$$\Delta_{np}(\rho) \simeq C_1 G(\rho) - C_2,$$

$$G(\rho) = \left(\frac{\langle \bar{q} q \rangle}{\langle \bar{q} q \rangle_0} \right)^{1/3}.$$

IN VACUUM,

$$\Delta_{np}(0) = m_n - m_p \simeq 1.29 \text{ MeV}.$$

Here, $\langle \bar{q} q \rangle$ and $\langle \bar{q} q \rangle_0$ are, respectively, the isospin averaged in-medium and in-vacuum chiral condensate. The coefficient C_1 is proportional to the u-d quark mass difference δm [1], through the isospin-breaking constant $\gamma \equiv \langle \bar{d} d \rangle_0 / \langle \bar{u} u \rangle_0 - 1$ as $C_1 = -a\gamma$ with a positive numerical constant a determined by the Borel QSR

method

Partial restoration of Chiral condensation of quark pairs $\bar{q}q$

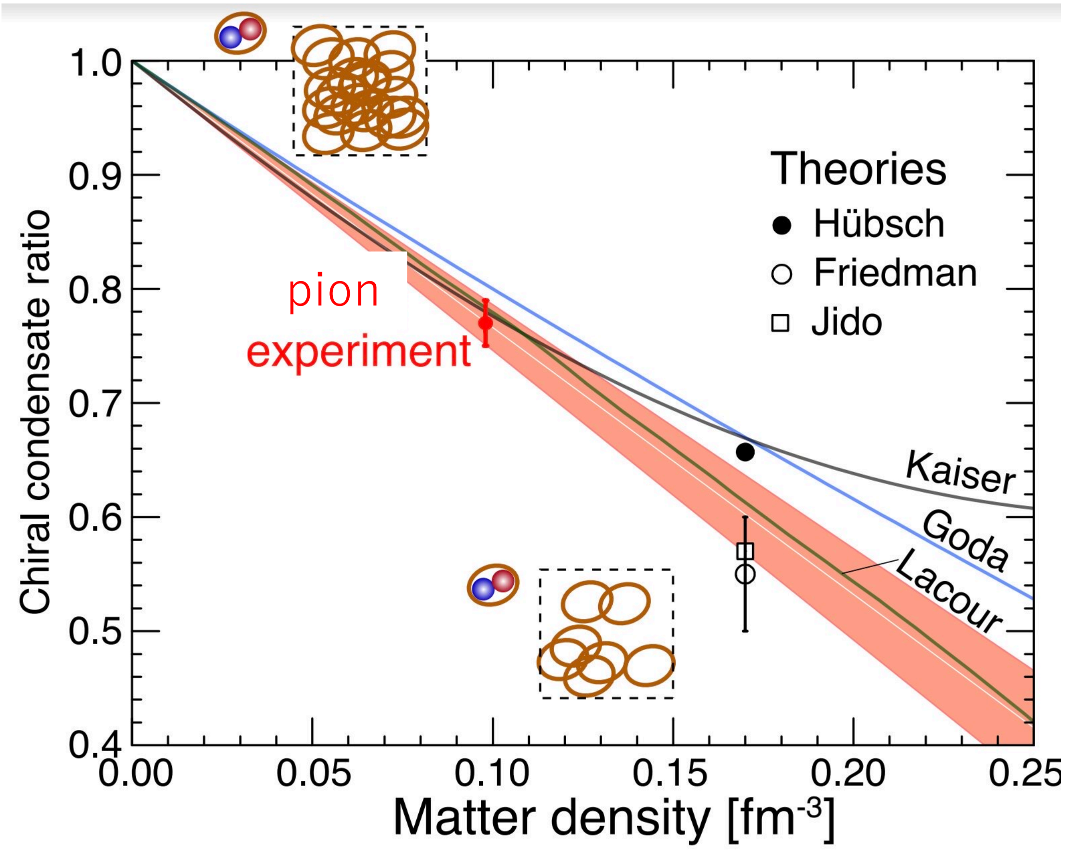

T. Nishi et al., Nature Physics, March 23, 2023
Pionic atom experiments

Goda and Jido

$$\frac{\langle \bar{q}q \rangle}{\langle \bar{q}q \rangle_0} \simeq 1 + k_1 \frac{\rho}{\rho_0} + k_2 \left(\frac{\rho}{\rho_0} \right)^{5/3}, \tag{2a}$$

$$k_1 = -\frac{\sigma_{\pi N} \rho_0}{f_\pi^2 m_\pi^2} < 0, \qquad k_2 = -k_1 \frac{3k_{F0}^2}{10 m_N^2} > 0, \tag{2b}$$

where $\sigma_{\pi N}$ is the π-N sigma term, m_π (m_N) is the pion (nucleon) mass, and f_π is the pion decay constant. The

The in-medium chiral condensate has a general form in the leading order of Fermi motion corrections;

The mass difference between (Z+/-1,N) and (Z, N+/-1) with N=Z

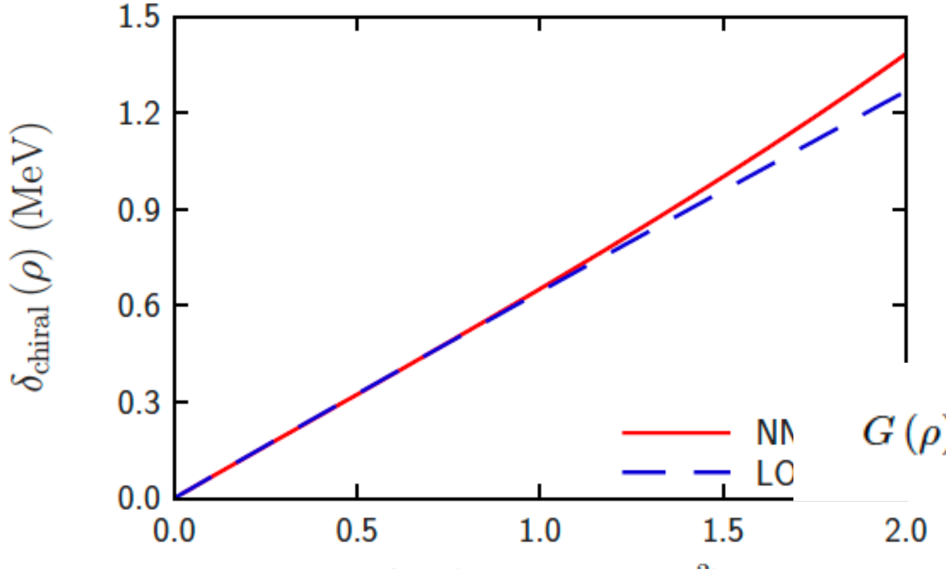

$$G(\rho) = \left(\frac{\langle \bar{q}q \rangle}{\langle \bar{q}q \rangle_0}\right)^{1/3}.$$

$$\frac{\langle \bar{q}q \rangle}{\langle \bar{q}q \rangle_0} \simeq 1 + k_1 \frac{\rho}{\rho_0} + k_2 \left(\frac{\rho}{\rho_0}\right)^{5/3}, \tag{2a}$$

$$k_1 = -\frac{\sigma_{\pi N}\rho_0}{f_\pi^2 m_\pi^2} < 0, \qquad k_2 = -k_1 \frac{3k_{\mathrm{F}0}^2}{10 m_N^2} > 0, \tag{2b}$$

where $\sigma_{\pi N}$ is the π-N sigma term, m_π (m_N) is the pion (nucleon) mass, and f_π is the pion decay constant. The

$$\tilde{s}_0 = -\frac{4}{3}\frac{C_1 \sigma_{\pi N}}{f_\pi^2 m_\pi^2}, \qquad \tilde{s}_1 + 3\tilde{s}_2 = \frac{1}{m_N^2}\frac{C_1 \sigma_{\pi N}}{f_\pi^2 m_\pi^2}.$$

The Skyrme-type CSB and CIB interactions

$$V_{\mathrm{CSB}}(\boldsymbol{r}) = \Big[s_0 (1 + y_0 P_\sigma) \delta(\boldsymbol{r}) + \frac{s_1}{2} (1 + y_1 P_\sigma) \left(\boldsymbol{k}^{\dagger 2} \delta(\boldsymbol{r}) + \delta(\boldsymbol{r}) \boldsymbol{k}^2 \right) + s_2 (1 + y_2 P_\sigma) \boldsymbol{k}^\dagger \cdot \delta(\boldsymbol{r}) \boldsymbol{k} \Big] \frac{\tau_{1z} + \tau_{2z}}{4},$$

$$\frac{E}{A} \simeq \varepsilon_0(\rho) + \varepsilon_1(\rho)\beta + \varepsilon_2(\rho)\beta^2.$$

$$\beta = (N - Z)/A$$

$$\Delta E = -2\varepsilon_1(\rho)$$

$$\delta_{\mathrm{Skyrme}} = -\frac{\tilde{s}_0}{4}\rho - \frac{1}{10}\left(\frac{3\pi^2}{2}\right)^{2/3} (\tilde{s}_1 + 3\tilde{s}_2)\rho^{5/3}, \tag{7}$$

where we have defined the effective coupling strengths,

$$\tilde{s}_0 \equiv s_0(1 - y_0), \quad \tilde{s}_1 \equiv s_1(1 - y_1), \quad \tilde{s}_2 \equiv s_2(1 + y_2). \tag{8}$$

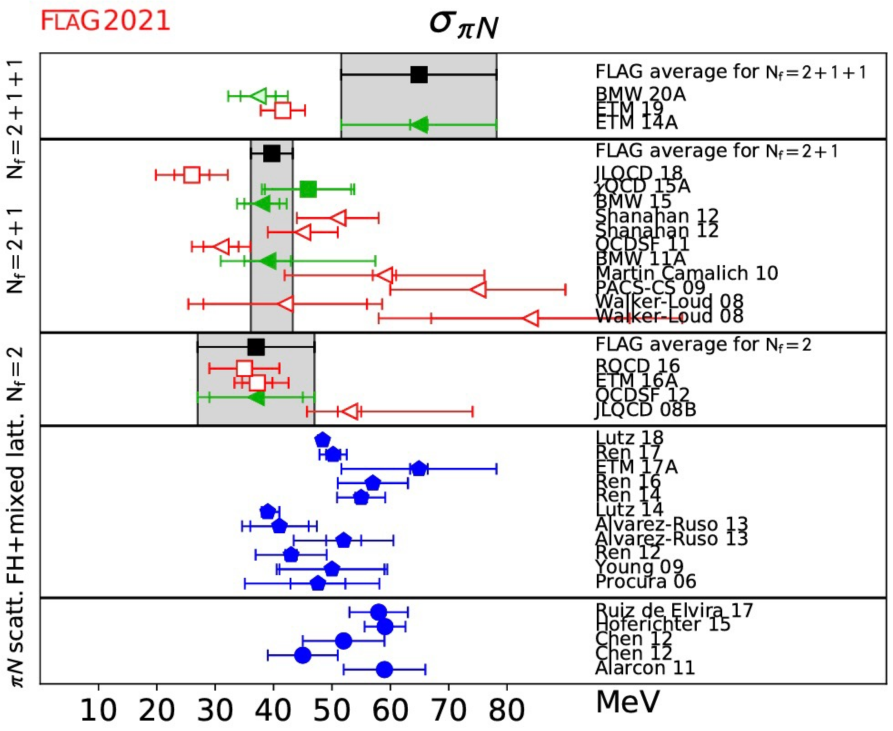

Figure 47: Lattice results and FLAG averages for the nucleon sigma term, $\sigma_{\pi N}$, for the $N_f = 2$, $2+1$, and $2+1+1$ flavour calculations. Determinations via the direct approach are indicated by squares and the Feynman-Hellmann method by triangles. Results from calculations which analyze more than one lattice data set within the Feynman-Hellmann approach [204, 211–219] are shown for comparison (pentagons) along with those from recent analyses of π-N scattering [186–188, 220] (circles).

a conservative estimate

$$\sigma_{\pi N} = 45 \pm 15 \text{ MeV}$$

TABLE II. Parameters of the Skyrme-type CSB interactions constrained from the low-energy constants in QCD. To evaluate the CSB effect in finite nuclei where $\tilde{s}_1$ and $\tilde{s}_2$ contribute independently, two characteristic parameter sets (Case I and Case II) are introduced.

$\tilde{s}_0$ (MeV fm^3)	$-15.5^{+8.8}_{-12.5}$	
$\tilde{s}_1+3\tilde{s}_2$ (MeV fm^5)	$0.52^{+0.42}_{-0.29}$	
	Case I	Case II
$\tilde{s}_0$ (MeV fm^3)	$-15.5^{+8.8}_{-12.5}$	$-15.5^{+8.8}_{-12.5}$
$\tilde{s}_1$ (MeV fm^5)	$0.52^{+0.42}_{-0.29}$	0.00
$\tilde{s}_2$ (MeV fm^5)	0.00	$0.18^{+0.14}_{-0.10}$

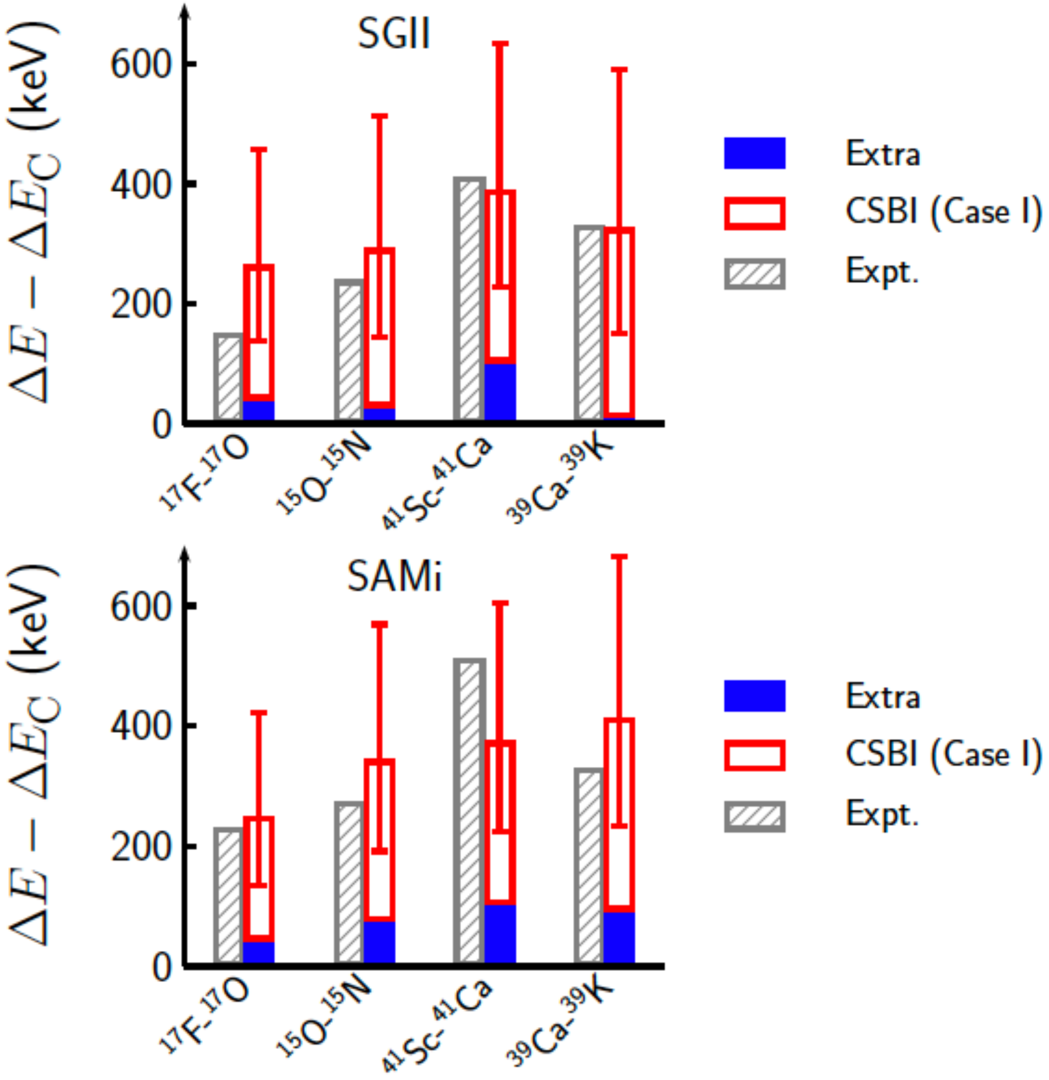

FIG. 2. Comparisons of the experimental ONS anomaly $\Delta E_{\rm Expt.} - \Delta E_{\rm C}$ (grey hatched bars) and the corresponding theoretical estimates in two EDFs (SGII and SAMi). The contribution from the QCD-based CSB interaction (CSBI) in Case I and the extra contributions are indicated by the red bars with error bars and the blue bars, respectively.

TABLE V. The breakdown of the mass difference of mirror nuclei ΔE into each contribution (Coulomb, Extra and CSB interaction (CSBI) for Case I with Skyrme EDF, SGII. Numbers are given in the unit of MeV.

Nuclei	^{17}F-^{17}O	^{15}O-^{15}N	^{41}Sc-^{41}Ca	^{39}Ca-^{39}K
Orbital	$1d_{5/2}$	$(1p_{1/2})^{-1}$	$1f_{7/2}$	$(1d_{3/2})^{-1}$
$\Delta E_{\rm D}$ (Coulomb)	3.596	3.272	7.133	6.717
$\Delta E_{\rm E}$ (Coulomb)	−0.203	0.026	−0.267	0.260
Extra	0.040	0.028	0.102	0.011
CSBI (Case I)	0.224	0.264	0.287	0.315
Sum (w/o CSBI)	3.432	3.326	6.965	6.985
Sum (w/ CSBI)	3.656	3.590	7.252	7.300
Expt. [29]	3.543	3.537	7.278	7.307

TABLE VI. The same as Table V, but with Skyrme EDF, SAMi.

Nuclei	^{17}F-^{17}O	^{15}O-^{15}N	^{41}Sc-^{41}Ca	^{39}Ca-^{39}K
Orbital	$1d_{5/2}$	$(1p_{1/2})^{-1}$	$1f_{7/2}$	$(1d_{3/2})^{-1}$
$\Delta E_{\rm D}$ (Coulomb)	3.506	3.242	7.025	6.697
$\Delta E_{\rm E}$ (Coulomb)	−0.193	0.022	−0.259	0.281
Extra	0.043	0.075	0.104	0.092
CSBI (Case I)	0.206	0.269	0.271	0.321
Sum (w/o CSBI)	3.356	3.339	6.870	7.070
Sum (w/ CSBI)	3.562	3.608	7.141	7.391
Expt. [29]	3.543	3.537	7.278	7.307

Summary

Gamow-Teller states of ^{48}Ca, ^{90}Zr, ^{132}Sn and ^{208}Pb are studied by SSRPA and 2p-2states make a larger spreading width with the proper excitation energies compared with experimental ones.

Quenching (SGII+Te1): ^{48}Ca ~35% Ex<20 MeV
^{208}Pb 30-40% Ex<25 MeV
Triplet-odd tensor plays an important role to increase the quenching

Excitation energy of magnetic dipole state is very sensitive to the triplet-odd tensor in RPA level, but the tensor effect is smacked in the SSRPA.

Beta decay life time has a strong effect by the 2p-2h correlations and also the tensor correlations.

Ab initio QCD-base CSB interaction is proposed for the first time and cures largely Okamoto-Nolen-Shiffer of the energydifference between mirror nuclei.

Collaborators

T. Naito, iTHEMS, RIKEN
T. Hatsuda, iTHEMS, RIKEN

Chunlin Bai, Sichun University, China
Mingjun Yang, Sichun Univerisity, China
H. Q. Zhang, CAEC, China

Xavi Roca-Maza, University of Milano, Italy

TABLE IV. Contributions from the Skyrme CSB interactions to $\delta_{\rm ONS}$ in Case I and Case II with theoretical uncertainties. The values are given in unit of keV. The core density and the wave function of valence orbit are calculated by HF model with Skyrme EDFs, SGII and SAMi. All the values are obtained self-consistently.

	Nuclei	^{17}F-^{17}O	^{15}O-^{15}N	^{41}Sc-^{41}Ca	^{39}Ca-^{39}K
	Orbital	$1d_{5/2}$	$(1p_{1/2})^{-1}$	$1f_{7/2}$	$(1d_{3/2})^{-1}$
SGII	$\tilde{s}_0$	229^{+192}_{-125}	269^{+221}_{-148}	292^{+245}_{-160}	322^{+264}_{-176}
	$\tilde{s}_1$ $(\tilde{s}_2 = 0)$	$-5.0^{+2.8}_{-4.0}$	$-5.6^{+3.1}_{-4.5}$	$-6.6^{+3.7}_{-5.3}$	$-6.0^{+3.4}_{-4.9}$
	$\tilde{s}_2$ $(\tilde{s}_1 = 0)$	$-6.4^{+3.5}_{-5.2}$	$-3.3^{+1.8}_{-2.7}$	$-5.3^{+2.9}_{-4.3}$	$-5.0^{+2.8}_{-4.1}$
	Case I	224^{+192}_{-125}	264^{+221}_{-148}	287^{+245}_{-160}	315^{+264}_{-176}
	Case II	225^{+192}_{-125}	266^{+221}_{-148}	289^{+245}_{-160}	316^{+264}_{-176}
SAMi	$\tilde{s}_0$	211^{+174}_{-115}	274^{+225}_{-152}	278^{+230}_{-151}	324^{+269}_{-180}
	$\tilde{s}_1$ $(\tilde{s}_2 = 0)$	$-5.2^{+2.9}_{-4.2}$	$-5.4^{+3.0}_{-4.4}$	$-7.3^{+4.0}_{-5.9}$	$-8.4^{+4.6}_{-6.6}$
	$\tilde{s}_2$ $(\tilde{s}_1 = 0)$	$-4.1^{+2.3}_{-3.3}$	$-3.2^{+1.8}_{-2.6}$	$-5.7^{+3.1}_{-4.6}$	$-5.2^{+2.9}_{-4.2}$
	Case I	206^{+174}_{-115}	269^{+225}_{-152}	271^{+230}_{-151}	321^{+269}_{-180}
	Case II	207^{+174}_{-115}	271^{+225}_{-152}	272^{+230}_{-151}	322^{+269}_{-180}

Nuclei	^{17}F-^{17}O	^{15}O-^{15}N	^{41}Sc-^{41}Ca	^{39}Ca-^{39}K
Particle (hole)	$1d_{5/2}$	$(1p_{1/2})^{-1}$	$1f_{7/2}$	$(1d_{3/2})^{-1}$
Finite size	−0.053	−0.070	−0.066	−0.082
Center-of-mass	0.023	0.030	0.014	0.018
$\delta^1_{\rm NN}$	0.014	0.006	0.034	0.021
$\delta^2_{\rm NN}$	0.050	−0.136	0.134	−0.176
Spin-orbit	−0.065	0.080	−0.126	0.142
pn mass difference	0.034	0.024	0.040	0.031
$\delta_{\rm pol}$	0.018	0.073	0.036	0.020
Vacuum polarization	0.019	0.021	0.036	0.037
Sum	0.040	0.028	0.102	0.011

TABLE S.II. The same as Table S.I, but for SAMi EDF.

Nuclei	^{17}F-^{17}O	^{15}O-^{15}N	^{41}Sc-^{41}Ca	^{39}Ca-^{39}K
Particle (hole)	$1d_{5/2}$	$(1p_{1/2})^{-1}$	$1f_{7/2}$	$(1d_{3/2})^{-1}$
Finite size	−0.050	−0.068	−0.063	−0.080
Center-of-mass	0.021	0.029	0.014	0.018
$\delta^1_{\rm NN}$	0.014	0.007	0.031	0.021
$\delta^2_{\rm NN}$	0.047	−0.090	0.131	−0.098
Spin-orbit	−0.061	0.078	−0.121	0.140
pn mass difference	0.035	0.026	0.041	0.034
$\delta_{\rm pol}$	0.018	0.073	0.036	0.020
Vacuum polarization	0.019	0.020	0.035	0.037
Sum	0.043	0.075	0.104	0.092